JOURNAL OF MATERIALS SCIENCE 29 (1994) 5699–5702

Localized boriding of low-carbon steel using a Nd:YAG laser

M. TAYAL, K. MUKHERJEE
Department of Materials Science and Mechanics, Michigan State University, East Lansing, MI 48824, USA

Localized boriding of low-carbon steel by the conventional technique requires tedious preboriding treatment and a long processing time. Laser boriding of low-carbon steel can be performed faster, and without any preboriding treatment. The feasibility of selective boriding of AISI 1018 steel using a Nd:YAG laser has been investigated. High hardness in the range 950–2200 H_V was obtained during laser boriding of AISI 1018 steel. The wide range of hardness is due to the variety of microstructures possible during laser boriding. Electron microprobe analysis showed that the highest hardness (2200 H_V) was due to the formation of FeB, and the lowest hardness was due to a mixture of Fe_2B and eutectic ($\alpha_{Fe} + Fe_2B$). The most desirable microstructure in laser boriding of AISI 1018 steel was found to be Fe_2B, which incorporates a combination of a high hardness, in the range of 1300–1700 H_V, and a compressive stress at the treated surface.

1. Introduction

Incorporation of boron into the surface of some metals or alloys results in the formation of metallic borides, which provide extremely hard wear-resistant, and erosion-resistant surfaces [1, 2]. In the past, boriding has been performed by means of a high-temperature electrolyte process [3], by pack boriding with boron-rich powder [4] and by gas-phase boriding [6]. All these processes are tedious and time consuming, especially if boriding is required at selective areas such as the inside of slots and grooves. Boriding, using a laser, appears to be a suitable technique for such applications, considering the focused energy of the laser and the flexibility in beam manipulation. The present work demonstrates the feasibility of selective boriding of AISI 1018 steel by using a Nd:YAG laser, and also presents a correlation between hardness and microstructures in laser-borided steel surfaces.

2. Experimental procedure

Laser boriding was carried out by using a 400 W Nd:YAG laser. AISI 1018 steel samples were in the shape of a rectangular plate (2.5 cm × 2.5 cm × 0.625 cm). Laser boriding was performed by moving boron powder-coated steel samples under a defocused (spot size 0.189 cm) laser beam. The traverse speed used for all boriding experiments was 2 mm s^{-1}. By varying the number of laser passes and boron powder-layer thickness, borided zones of various thickness, and with different microstructures were obtained. After laser boriding, both longitudinal and transverse sections of samples were cut and prepared for microstructural examination. Microstructural investigation was carried out using an Olympus optical microscope, and a Hitachi S-2500C scanning electron microscope (SEM). Phase, and composition analysis of laser-borided samples were performed using a Scintag X-ray diffractometer, and an electron microprobe (Applied Research Laboratories, Inc.,). A series of laser-borided samples with different microstructures was studied to determine the influence of composition on the borided surface properties, such as hardness and resistance to cracking.

3. Results and discussion

A typical micrograph of the transverse section of laser-borided track is shown in Fig. 1. This micrograph shows excellent bonding of the borided layer to the substrate metal. The microstructure consists of Fe_2B dendrites in eutectic (α_{Fe}-Fe_2B). The process cycle for the microstructure shown in Fig. 1 consisted in two passes of the laser beam (7.13×10^3 W cm^{-2}) on the boron-coated (0.18 mm) sample. Different microstructures evolved during laser boriding were controlled by varying the thickness of the boron powder layer and the power density of the laser. Microstructure, in turn, controlled the hardness profile across the borided zone. Fig. 2 shows the hardness profiles of laser-borided specimens, treated under different combinations of process parameters. These profiles show the effect of various microstructures, formed under different conditions of laser process parameters, on the hardness distribution at the borided zone. A notation system of x–y–p–t has been used to denote processing parameters in Fig. 2, where x denotes the number of times the boron coating was applied, y denotes the number of laser passes, p denotes the laser power (W)

0022–2461

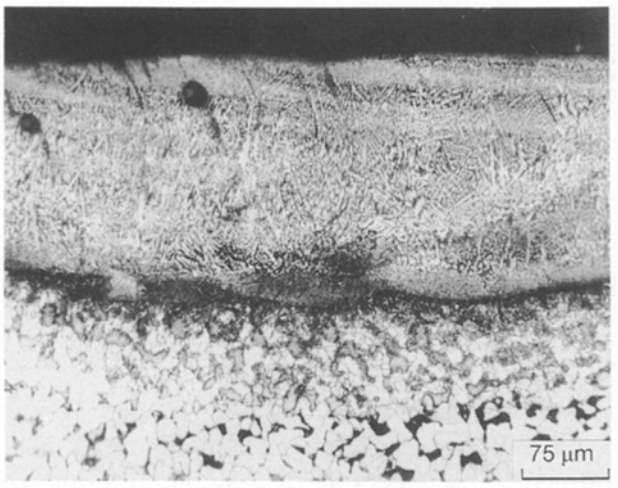

Figure 1 A typical scanning electron micrograph of a transverse section of a laser-borided zone.

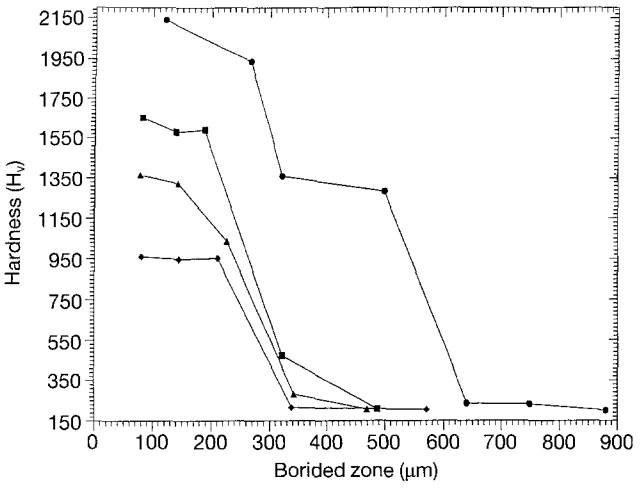

Figure 2 Hardness profiles at the transverse section of laser-borided samples treated under different processing conditions. The symbols denote x–y–p–t, where x is the number of boron coating times, y is the number of laser passes, p is the laser power (W) (power density = $35.64 \times p$ W cm^{-2}), and t is the thickness (mm) of the boron coating. (◆) 1–2–200–0.18, (▲) 1–2–200–0.28, (■) 2–2–200–0.38, (●) 3–3–200–0.38.

(power density = $35.64 \times p$ W cm^{-2}) and t is the thickness (mm) of boron coating. Highest hardness has been achieved for a case in which $x = 3$, $y = 3$, $p = 200$ W (7.13×10^3 W cm^{-2}) and $t = 0.38$ mm. The high hardness of 2150 H_v matched the hardness of the single-phase FeB. The lowest hardness of 950 H_v was observed for a case in which $x = 1$, $y = 2$, $p = 200$ W (7.13×10^3 W cm^{-2}) and $t = 0.18$ mm. This lower hardness was similar to that of a single-phase eutectic (α_{Fe} + Fe_2B). Increasing the saturation of boron in the borided zone, resulted in the hardness profiles (shown in Fig. 2) for samples 1–2–200–0.28 and 2–2–200–0.38. For the sample 1–2–200–0.28, the microstructure consisted of mostly Fe_2B, whereas in sample 2–2–200–0.38, which has a hardness in between the hardness of samples 3–3–200–0.38 and 1–2–200–0.28, the microstructure consisted of mixture of Fe_2B and FeB.

X-ray analysis of a laser-borided sample, which was treated with two passes of the laser beam, and two successive layers of boron coatings, showed (Fig. 3) diffraction peaks representative of stable FeB and Fe_2B phases, although some peaks corresponding to metastable phase Fe_3B [7] have also been observed. The formation of the metastable phase Fe_3B can be explained by the non-equilibrium cooling conditions, prevalent during laser surface treatments. Fig. 3 shows the evidence of texture formation in the laser-borided zone. Both FeB and Fe_2B phases exhibited a sharp texture. The FeB was found to be preferentially oriented in ⟨1 1 1⟩ texture, whereas the Fe_2B phase shows a ⟨0 0 2⟩ texture. The degree of texture in Fe_2B was studied using the ratio, R, of the diffracted intensities corresponding (0 0 2) and (2 0 1) peaks. For a randomly oriented Fe_2B, the value of R is 0.25. The value of R was found to be 0.67 for Fe_2B (from Fig. 3) in the borided zone, indicating a significant texture. In addition to Fe_2B, FeB has also been found to have a significant texture. The degree of texture in FeB was determined by using the intensity ratio of the (1 1 1) and (0 2 1) diffraction peaks. The value of R was found to be 1.5 for FeB (from Fig. 3), compared to the ratio of 0.72, for randomly oriented FeB.

The concentration of boron in laser-borided zones was determined by using an Applied Research Laboratories microprobe. The measurements for B K_α were obtained using lead stearate crystal (Pb–St) detector. Fig. 4 shows the boron and iron mapping of a transverse section of a laser-borided specimen. It shows two phases: one phase richer in boron than the other phase. Individual total counts for boron in each phase were used to approximate the composition of the phase. The boron-rich phase (16.3 wt % B) was found to be approximately matching the composition of FeB (16.9 wt%) [5]. The composition of boron-deficient phases was found to match approximately the composition of a peritectically formed Fe_2B. Fig. 5 shows the boron and iron mapping in the area interior to the one shown in Fig. 4. The microstructure in Fig. 5 shows more of a boron-deficient phase than the boron-rich phase. Boron mapping in Fig. 4 (surface) and 5 (subsurface) proves a gradual decrease in boron

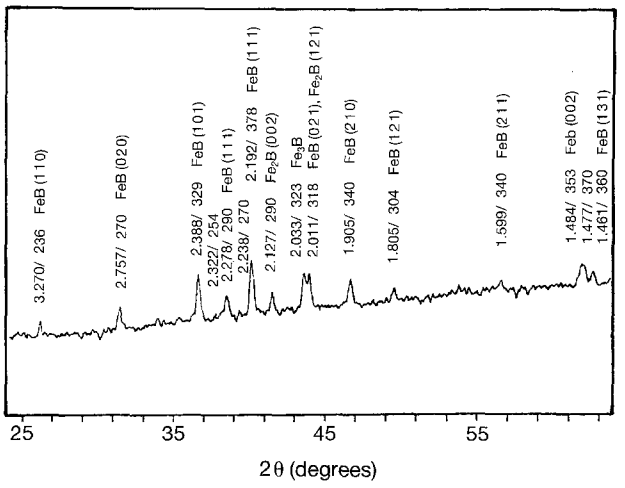

Figure 3 X-ray diffraction diagram of a laser-borided zone.

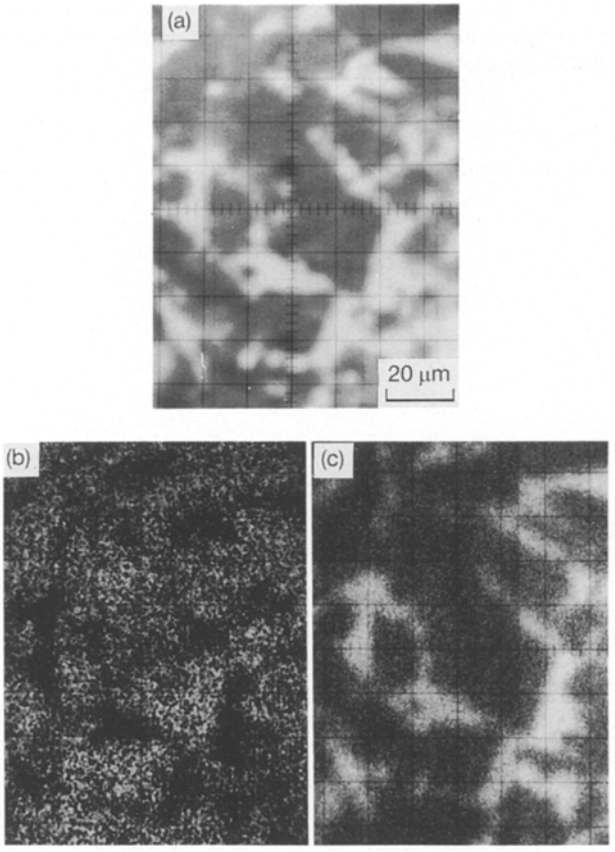

Figure 4 Micrograph showing boron and iron mapping in an area at the surface (in transverse section) of a laser-borided sample: (a) microstructure, (b) boron mapping, (c) iron mapping.

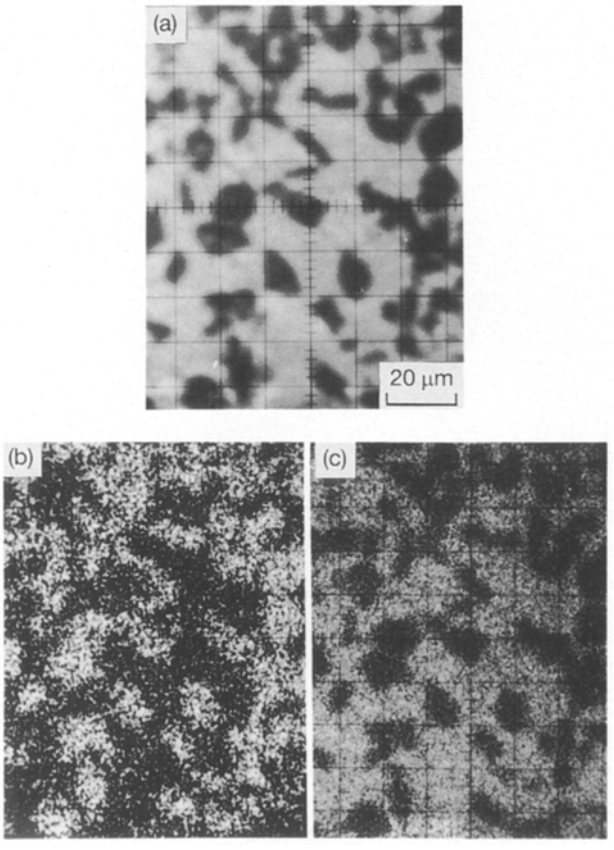

Figure 5 Micrograph showing boron and iron mapping in an area 110 μm inside the surface (in transverse section) of a laser-borided sample: (a) microstrcture, (b) boron mapping, (c) iron mapping.

TABLE I Thermal expansion coefficients ($10^6 K^{-1}$) [8, 9]

FeB	15.0
Fe_2B	8.0
Fe	12.0

concentration from the borided surface inwards. A gradual decrease in boron concentration, compared to a sharp drop, leads to good bonding between the boride coating and the substrate.

Cracks were observed in borided zones which had almost 100% FeB phase. No cracks, however, were detected in the borided zones with the Fe_2B phase. The crack formation in the borided layer is thought to be due to the thermal stresses, because no solidification cracking was observed. One of the important variables controlling the magnitude of the thermal stress, is the thermal expansion coefficient. After examining the thermal expansion coefficients (Table I) of FeB, Fe_2B and iron, important information can be extracted. If the surface of the laser-borided sample contains mostly FeB phase, then the surface will try to contract much more during cooling than the sample with only Fe_2B phase or steel. Therefore, the result will be a tensile stress and the sample will be more prone to cracking. On the other hand, the coefficient of expansion of Fe_2B is less than that of steel, and hence it contracts less during cooling. This puts the Fe_2B layer in a compressive state after cooling. This analysis, together with the experimental results of laser boriding, demonstrates that the best microstructure in the laser-borided layer should be the single-phase Fe_2B. Fe_2B in the microstructure imparts ideal properties to the laser-borided layer: a high hardness (1300–1600 H_v) and a favourable state of compressive stress.

4. Conclusion

Selective boriding of AISI 1018 steel using a Nd:YAG laser has been investigated. The high surface hardness of laser-borided AISI steel was due to the formation of FeB and Fe_2B phases. The surface hardness observed was in the range 950–2200 H_v. The desirable microstructure for laser boriding of AISI 1018 steel is the single-phase Fe_2B, which imparts ideal properties to the borided layer : high hardness (1300–1600 H_v) and a favourable state of compressive stress in the surface layer.

References

1. W. LILIENTAL, in "Wear of Materials 1983", edited by K. C. Ludema (ASME, New York, 1983) p. 556.
2. A. P. EPIK, in "Boron and Refractory Borides", edited by V. I. Matkovich (Springer, New York, 1977) p. 597.
3. N. S. ZINOVICH, in "Diffusion Cladding of Metals", edited by G. V. Samsonov (Consultants Bureau, New York, 1967) p. 43.
4. I. S. DUKAREVICH and M. A. BALTER, in "Protective Coatings on Metals I", edited by G. V. Samsonov (Consultant Bureau, New York, 1969) p. 30.

5. O. KUBASCHEWSKI, "Iron-Binary Phase Diagrams" (Springer, New York, 1982) p. 15.
6. P. GOEURIOT, F. THEVENOT, J. H. DRIVER and T. MAGNIN, in "Advances in Surface Treatment", edited by A. Niku-lari (Springer, New York, 1990) p. 171.
7. Y. KHAN, E. KNELLER and M. SOSTARICH, *Z. Metallkde* **73** (1982) 624.
8. Z. Z. LIN, Z. M. LING and X. C. SUN, in "Wear of Materials 1989", edited by K. C. Ludema (ASME, New York, 1989) p. 51.
9. T. S. EYRE, *Wear* **34** (1975) 383.

Received 11 May 1993
and accepted 28 April 1994